*Journal of Organometallic Chemistry*, 412 (1991) 177–193
Elsevier Sequoia S.A., Lausanne
JOM 21735

# A comparison of the clusters $[Os_3(\mu\text{-H})(\mu\text{-X})(CO)_{10}]$ where X is furyl, thienyl, pyrrolyl, or indolyl: *monohapto* versus *dihapto* and *exo* versus *endo* coordination

Alejandro J. Arce *, Jorge Manzur, Manuel Marquez, Ysaura De Sanctis

*Chemistry Centre, Instituto Venezolano de Investigaciones Cientificas (IVIC), Apartado 21827, Caracas 1020-A (Venezuela)*

and Antony J. Deeming *

*Department of Chemistry, University College London, 20 Gordon Street, London WC1H 0AJ (UK)*

(Received January 3rd, 1991)

**Abstract**

The thienyl complexes $[Os_3(\mu\text{-H})(\mu\text{-}C_4H_2RS)(CO)_{10}]$ (**1**, R = H and **2**, R = Me) were synthesised through the reactions of thiophene or 2-methylthiophene with $[Os_3(CO)_{10}(MeCN)_2]$, which lead to C–H bond activation adjacent to the sulphur atom. The crystal structure when X = Me shows that the thienyl ligand is $\mu,\eta^2$-bonded, although the distance between an Os atom and the $\beta$-carbon is particularly long (Os(2)–C(2) 2.82(3) Å), longer than the corresponding distance in the previously reported furyl complex **3** (2.63(1) Å). The presence and interconversion of *exo* and *endo* isomers of these complexes in solution are described. The interconversion mechanism is believed to involve a transient heteroatom-bonded intermediate. *N*-Methylpyrrole similarly gives the stoichiometrically equivalent but structurally different cluster $[Os_3(\mu\text{-H})(\mu\text{-}C_4H_3NMe)(CO)_{10}]$ (**5**) but in this case the crystal structure shows that the pyrrolyl ring is perpendicular to the $Os_3$ ring and is $\mu,\eta^1$-coordinated. Attempts to synthesise the directly analogous indol-2-yl complex, which we predict should be $\mu,\eta^2$-coordinated, like the furyl and thienyl compounds, led instead to the indol-3-yl isomer $[Os_3(\mu\text{-H})(\mu\text{-}C_6H_4C_2HNMe)(CO)_{10}]$ (**6**), again with vertical $\mu,\eta^1$-coordination, as shown by its crystal structure. A structural comparison of these compounds is presented.

## Introduction

Alkyne ligands coordinated in the $\mu_3,\eta^2$-mode (**A**) and vinyl ligands in the $\mu,\eta^2$-mode (**C**) (Fig. 1) are commonly found in a wide range of polynuclear organotransition metal chemistry. However, heteroatom substituents can have a major effect on the nature of the metal–ligand bonding. An example from our own work is the replacement of MeO by $Et_2N$ in the clusters $[Os_3(\mu\text{-H})_2(\mu_3\text{-CHCX})(CO)_9]$ (X = MeO [1] or $Et_2N$ [2,3]), which leads to the change from the parallel form (**A**) to the perpendicular form (**B**) (Fig. 1), that is with the C–C bond rotated from parallel to perpendicular to a metal–metal edge. This is a consequence

0022-328X/91/$03.50 

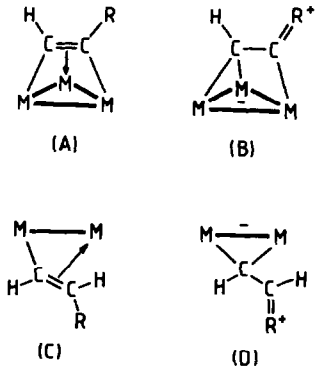


Fig. 1. Possible modes of attachment of the alkyne ligands CHCX to three metal atoms and of the vinyl ligands CHCHX to two metal atoms.

of the more effective $\pi$-donation by the amino group than by the alkoxy substituent. Likewise the vinyl ligand CH=CHR (R = OEt) in $[Os_3(\mu\text{-H})(\mu\text{-CHCHR})(CO)_{10}]$ adopts the $\mu,\eta^2$-coordination mode (**C**) [4], whereas Shapley et al. have shown that the ligand $CHCHNEt_2$ (R = $NEt_2$) forms the $\mu,\eta^1$-system with an alkylidene bridge as in **D** [5]. Again the strong $\pi$-donor ability of the amino group leads to a redistribution of the $\pi$-electrons and the formation of the lower hapticity system.

In this paper we report on related heteroatom effects in the heterocyclic complexes of the type $[Os_3(\mu\text{-H})(\mu\text{-}C_4H_3X)(CO)_{10}]$ (X = O, S, NMe) derived from furan, thiophene, and *N*-methylpyrrole. The effects of introducing the benzo group by using *N*-methylindole are also described.

## Results and discussion

*Thienyl clusters*

Reactions of thiophene or 2-methylthiophene with $[Os_3(CO)_{10}(MeCN)_2]$ result in the breakage of C–H bonds next to the S-atom and the formation of the $[Os_3(\mu\text{-H})(\mu\text{-}C_4H_2RS)(CO)_{10}]$ (**1**, R = H and **2**, R = Me) [6]. These thienyl compounds may be compared with the furyl complex previously reported to be formed in a similar way from furan: $[Os_3(\mu\text{-H})(\mu\text{-}C_4H_3O)(CO)_{10}]$ (**3**) [7] (see Table 1 for IR and NMR data). We have also synthesised the 2-methylfuryl derivative **4** by the same method. There has been interest recently in the transition-metal chemistry of thiophene because of the commercial importance of the hydrodesulphurization (HDS) process, sulphur being substantially incorporated in thiophenic type rings in crude oil. Thiophene, in general, does not readily coordinate to transition metals, even to soft class b metals, but nevertheless compounds with thiophene coordinated in various ways have been reported (see ref. 8 for some examples). We have reported that thiophene can be incorporated in its dehydrogenated form in the cluster $[Os_3(\mu\text{-H})_2(\mu_3\text{-}C_4H_2S)(CO)_9]$, the structure of which was reported [9]. However, this present report describes for the first time the formation of a coordinated thienyl ligand directly by metallation of thiophene; our previous work involved the oxidative addition of 2-formylthiophene at the aldehyde function followed by decarbonylation.

Table 1

IR and $^1$H NMR data for the complexes $[Os_3(\mu\text{-H})(\mu\text{-X})(CO)_{10}]$, clusters **1** to **6**

| Compound | X | $\nu$(CO) [a] ($cm^{-1}$) | $^1$H NMR [b] | |
|---|---|---|---|---|
| **1** [c] | $C_4H_3S$ | 2104w 2066vs | **1a** *exo* (80%) | **1b** *endo* (20%) |
| | | 2053s 2020vs | 8.36 (d, $H^x$) $J_{xy}$ 5.2 | 9.26 (d, $H^x$) $J_{xy}$ 4.3 |
| | | 2009s 1993m | 7.46 (d, $H^z$) $J_{yz}$ 3.2 | 8.69 (d, $H^z$) $J_{yz}$ 3.6 |
| | | 1983w | 6.86 (m, $H^y$) | 7.35 (dd, $H^y$) |
| | | | −15.21 (s, $H^w$) | −14.41 (s, $H^w$) |
| **2** [d] | 2-$MeC_4H_2S$ | 2103w 2064vs | **2a** *exo* (67%) | **2b** *endo* (33%) |
| | | 2052s 2018vs | 7.64 (d, $H^x$) $J_{xy}$ 3.0 | 8.52 (d, $H^x$) $J_{xy}$ 3.6 |
| | | 2008vs 1992m | 6.55 (d, $H^y$) | 7.07 (d, $H^y$) |
| | | 1982w | 2.38 (s, Me) | 2.32 (s, Me) |
| | | | −15.12 (s, $H^w$) | −14.66 (s, $H^w$) |
| **3** [e] | $C_4H_3O$ | 2107w 2071vs | **3a** *exo* (90%) | **3b** *endo* (10%) |
| | | 2058s 2023vs | 7.84 (d, $H^x$) $J_{xy}$ 3.3 | 8.10 (d, $H^x$) $J_{xy}$ 3.6 |
| | | 2009s 2004m | 7.40 (d, $H^z$) $J_{yz}$ 1.9 | 7.93 (d, $H^z$) $J_{yz}$ 1.5 |
| | | 2000m 1992w | 5.33 (dd, $H^y$) | 5.53 (dd, $H^y$) |
| | | 1986w | −15.53 (s, $H^w$) | −14.78 (s, $H^w$) |
| **4** [e] | 2-$MeC_4H_2O$ | 2103w 2065vs | **4a** *exo* (85%) | **4b** *endo* (15%) |
| | | 2053s 2017vs | 8.55 (d, $H^x$) $J_{xy}$ 3.3 | 8.72 (d, $H^x$) $J_{xy}$ 3.5 |
| | | 2005s 1997s | 6.06 (d, $H^y$) | 6.40 (d, $H^x$) |
| | | 1982w | 2.10 (s, Me) | 1.95 (s, Me) |
| | | | −15.16 (s, $H^w$) | −14.76 (s, $H^w$) |
| **5** [e] | $C_4H_3NMe$ | 2100m 2058vs | 8.60 (dd, $H^x$) $J_{xy}$ 1.2 | |
| | | 2046s 2017vs | 8.21 (m, $H^y$) $J_{yz}$ 2.3 | |
| | | 2005s 1982sh | 6.43 (dd, $H^z$) $J_{xz}$ 4.2 | |
| | | 1978s | −15.20 (s, $H^w$) | |
| **6** [e] | $C_8H_5NMe$ | 2096m 2055vs | 8.80 (s, $H^x$) | |
| | | 2044s 2014vs | 7.35 (m, $C_6H_4$) | |
| | | 1955s 1985m | 3.75 (s, Me) | |
| | | 1974w | −14.73 (s, $H^w$) | |

[a] Recorded in cyclohexane. [b] NMR in $CD_2Cl_2$ (300 MHz). [c] −55 °C. [d] −50 °C. [e] Room temperature.

Crystals of $[Os_3(\mu\text{-H})(\mu\text{-}C_4H_2MeS)(CO)_{10}]$ (**2**) suitable for single-crystal structure determination were obtained and the molecular structure is shown in Fig. 2. Selected bond lengths and angles are in Table 2. The structure is closely related to that of the reported furyl compound **3** [7] with the ligand coordinated in a $\mu,\eta^2$-manner. The dihedral angle between the $C_4S$ and the $Os_3$ planes is 55.4°. The distance between the $\beta$-carbon atom and the nearest osmium atom is long (Os(2)–C(2) 2.82(3) Å) and would be considered non-bonding under most circumstances. Osmium–carbon bond lengths are below 2.0 Å when there is multiple bonding as in metal carbonyls, and lengths of 2.1 to 2.2 Å are commonly found for Os–C $\sigma$-bonds. In $\eta^n$-complexes such distances are typically 2.2 to 2.4 Å, but a much longer distance is found in **2**. In the furyl compound, this distance is shorter but still long (2.63(1) Å), while in the related parent vinyl compound $[Os_3(\mu\text{-H})(\mu\text{-}CH{=}CH_2)(CO)_{10}]$ it is much shorter (2.362(3) Å) [10,11]. This considerable variation in the geometries of $\mu,\eta^2$-type bridges will be discussed later.

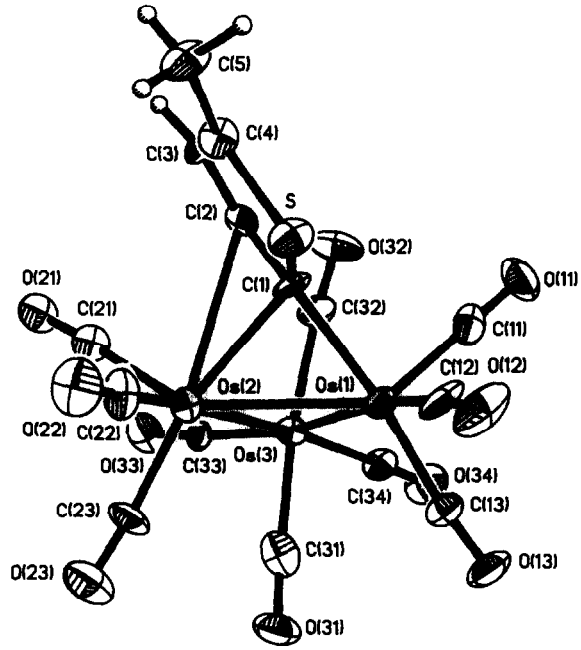


Fig. 2. Molecular structure of the thienyl cluster $[Os_3(\mu\text{-H})(\mu\text{-}C_4H_2MeS)CO)_{10}]$ (**2**) showing the $\mu,\eta^2$-attachment of the thienyl ligand.

A very interesting feature of compounds **1** and **2** is that the $^1H$ NMR spectra show the presence of isomers (Table 1). The spectrum of $[Os_3(\mu\text{-H})(\mu\text{-}C_4H_3S)(CO)_{10}]$ (**1**) at room temperature (27 °C) shows four very broad resonances for the four distinct H atoms (Fig. 3). At −55 °C these broad resonances have resolved into 8 resonances (four weak signals at $\delta$ 9.26, 8.69, 7.35, and −14.41 for isomer **1b** (20%) and four strong signals at $\delta$ 8.36, 7.46, 6.86, and −15.21 for isomer **1a** (80%)). Figure 3 shows how the rapid exchange of these isomers leads to coalescence. We

Table 2

Selected bond lengths (Å) and angles (°) for the cluster $[Os_3(\mu\text{-H})(\mu\text{-}C_4H_2MeS)(CO)_{10}]$ (**2**)

| | | | |
|---|---|---|---|
| Os(1)–Os(2) | 2.816(2) | C(1)–C(2) | 1.42(3) |
| Os(1)–Os(3) | 2.859(2) | C(2)–C(3) | 1.37(4) |
| Os(2)–Os(3) | 2.883(2) | C(3)–C(4) | 1.33(4) |
| Os(1)–C(1) | 2.15(3) | C(4)–C(5) | 1.42(4) |
| Os(2)–C(1) | 2.35(3) | C(4)–S | 1.72(3) |
| Os(2)–C(2) | 2.82(3) | Os(1)···S | 3.35(3) |
| Os(1)···C(2) | 3.35(3) | Os(2)···S | 3.53(3) |
| C(1)–S | 1.78(3) | | |
| Os(1)–Os(2)–Os(3) | 60.2(1) | Os(1)–Os(2)–C(1) | 48.1(6) |
| Os(1)–Os(3)–Os(2) | 58.7(1) | Os(2)–Os(1)–C(1) | 54.6(7) |
| Os(2)–Os(1)–Os(3) | 61.1(1) | Os(1)–C(1)–Os(2) | 77.3(9) |
| Os(3)–Os(1)–C(1) | 91.9(7) | Os(1)–C(1)–S | 117(1) |
| Os(3)–Os(2)–C(1) | 87.3(7) | Os(2)–C(1)–S | 117(1) |

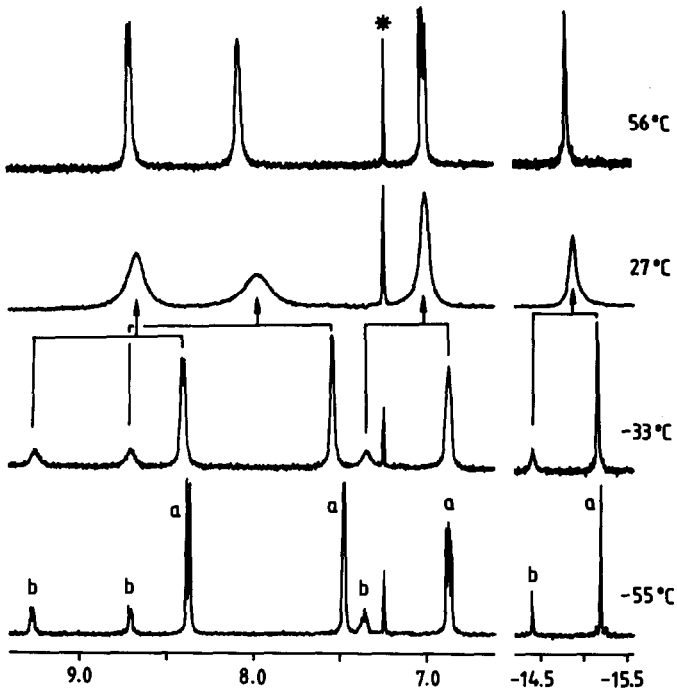


Fig. 3. $^1$H NMR spectra of the thienyl cluster $[Os_3(\mu\text{-H})(\mu\text{-}C_4H_3S)(CO)_{10}]$ (**1**) in $CDCl_3$ solution. Signals of the *exo* isomer are marked a and those of the *endo* isomer are marked b; the $CHCl_3$ singlet is marked ★.

assume that the major isomer is that which crystallises and for which the structure was determined but there is the question of the nature of the minor isomer. We thought that the isomers might have the heteroatom *exo* or *endo* with respect to the $Os(CO)_4$ group respectively, although there was a possibility that the minor isomer **1b** might be the *S*-bonded form. We re-examined the reported furyl compound **3** and also synthesised its analogue **4** from 2-methylfuran to establish the differences between the oxygen- and sulphur-containing heterocycles, since major differences between the O and S systems should be clearly apparent if heteroatom coordination is involved. Isomers of the furyl analogue $[Os_3(\mu\text{-H})(\mu\text{-}C_4H_3O)(CO)_{10}]$ (**3**) were not described in the original report [7], but we now find that clusters **1** to **4** all exist as isomers in solution. In the case of the furyl compounds the minor isomers are somewhat lower in relative concentration than for the thienyl compounds (80% (**1a**); 20% (**1b**); 67% (**2a**); 33% (**2b**); 94% (**3a**); 6% (**3b**); 85% (**4a**); 15% (**4b**)) and it is just possible that the 6% of the minor isomer **3b** of the furyl compound was not observed or ignored in the original study. We do not believe that these observed changes in the population distributions on replacing S by O atoms are consistent with these isomers having the heteroatom coordination to osmium. A much stronger preference for *S*-coordination over *O*-coordination was expected. However, an obvious difference between the furyl complexes **3** and **4** and the thienyl complexes **1** and **2** is that the isomers give separate signals even at 75 °C (Fig. 4). At this temperature the signals for the minor isomer have just started to broaden whereas those of the major isomer still exhibit fine structure. The onset of exchange would be apparent in the

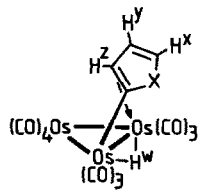

(1a) (X = S)
(3a) (X = O)

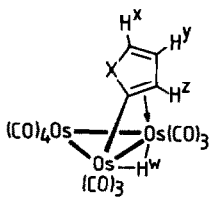

(1b) (X = S)
(3b) (X = O)

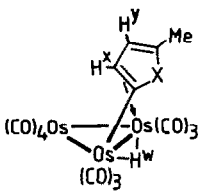

(2a) (X = S)
(4a) (X = O)

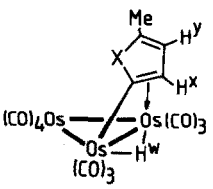

(2b) (X = S)
(4b) (X = O)

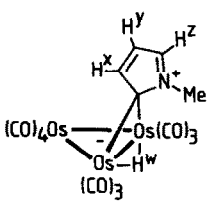

(5)

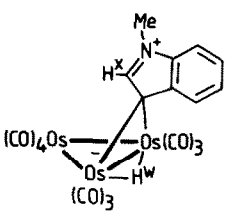

(6)

weaker signals first. We estimate that the coalescence temperatures for the furyl compounds are at least 100 °C higher than for the thienyl compounds. This represents something like a $10^3$-fold faster rate for the thienyl than for the furyl complex, although we did not make a complete kinetic analysis of the system.

In the light of these results for the thienyl compounds **1** and **2** and the furyl compounds **3** and **4**, we propose that the minor isomers of each are the *endo* isomers rather than the heteroatom-coordinated forms and the major isomers are *exo* as in the crystals. The dynamic behaviour therefore is the first example of an *exo* to *endo* conversion in a system of this kind. It is well known that $\mu,\eta^2$-vinyl ligands, such as in $[Os_3(\mu\text{-H})(\mu\text{-CH=CH}_2)(CO)_{10}]$, can rapidly oscillate between the metal atoms by interchanging the $\sigma$ and $\eta^2$ bonding to the bridged metal atoms. Opposite faces of the ligand become successively employed in the $\eta^2$-coordination as the ligand passes through a transition state with the ligand plane perpendicular to the metal plane. We presume this is occurring for compounds **1** to **4**, but this is not the process that leads to *exo–endo* conversion. Isomers of this kind have not been observed with acyclic vinyl ligands, although the different geometries have been observed in different compounds, structure **E** when the vinyl is CH=CHR and structure **F** when it is CPh=CHPh (Fig. 5) [12]. A clash of the Ph substituent at the $\alpha$ position with an axial CO ligand would destabilise structure **E** for the CPh=CHPh complex. In the

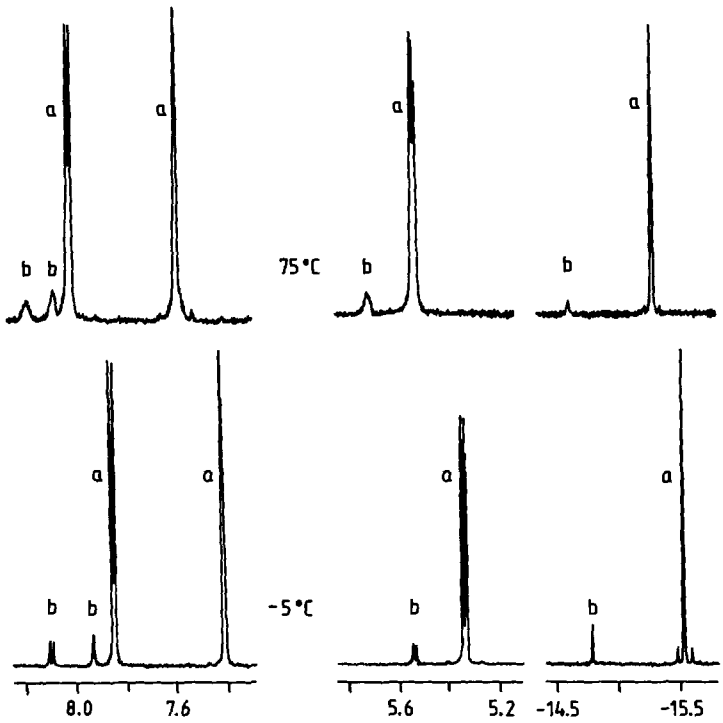


Fig. 4. $^1$H NMR spectra of the furyl cluster $[Os_3(\mu\text{-}H)(\mu\text{-}C_4H_3O)(CO)_{10}]$ (3) in $C_6D_6$ solution. Signals of the *exo* isomer are marked a and those of the *endo* isomer are marked b.

cyclic systems described here there is little to favour one isomer over the other on steric grounds and both are observed in equilibrium. We do not know whether the heteroatoms are essential for rapid interconversion. If they are necessary, it is very likely that the mechanism involves an intermediate with a coordinated heteroatom. The much greater rate for the thienyl compared with the furyl systems is then consistent with this mechanism (Scheme 1) and we predict that a purely hydrocarbon system such as $\mu,\eta^2$-cyclopentenyl would not undergo this process, at least, not by the same pathway.

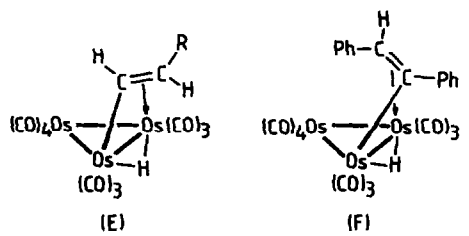


Fig. 5. Known modes of attachment of vinyl ligands in the clusters $[Os_3(\mu\text{-}H)(\mu\text{-vinyl})(CO)_{10}]$ where vinyl = CH=CHR (**E**) and PhC=CHPh (**F**).

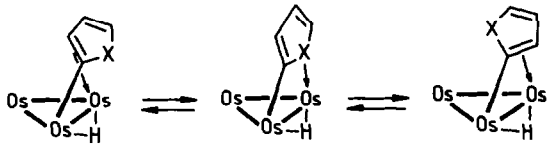

Scheme 1

*N-Methylpyrrolyl cluster*

The IR spectrum of the *N*-methylpyrrolyl complex $[Os_3(\mu\text{-}H)(\mu\text{-}C_4H_3NMe)(CO)_{10}]$ (**5**), directly analogous to clusters **1** and **3**, has $\nu(CO)$ absorptions at rather lower wavenumbers than do compounds **1** to **4** indicating that the $\pi$-donor properties of the NMe group are operating. We considered that the compound might be a $\mu$-alkylidene system related to the cluster $[Os_3(\mu\text{-}H)(\mu\text{-}CHCHNEt_2)(CO)_{10}]$ [5] and determined the crystal structure to test this. The structure is shown in Fig. 6 and selected bond lengths and angles are in Table 3. The angle between the $C_4N$ ring and the $Os_3$ plane is 90.6° and C(2) is non-bonded to the metal atoms (Os(1)–C(2) 3.19(2) and Os(2)–C(2) 3.19(2) Å). Figure 7 shows two ways the *N*-methylpyrrolyl ligand could coordinate, **G** and **H**, and we believe that **H** is a closer representation of the real system than **G**. Thus replacement of S in **1** or O in **3** by NMe has had a significant structural consequence.

We considered that, since form **H** is favoured over form **G**, it might be possible to tilt the balance in favour of form **G** by introducing a benzo ring. The corresponding product from *N*-methylindole would likely adopt the structure **I** in preference to that of **J** (Fig. 7) because the latter quinoidal form is expected to be relatively

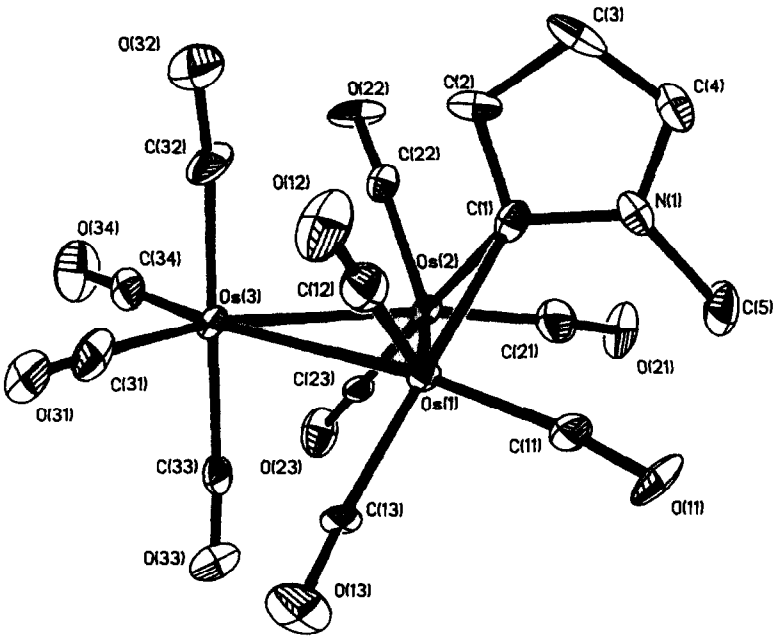


Fig. 6. Molecular structure of the *N*-methylpyrrolyl cluster $[Os_3(\mu\text{-}H)(\mu\text{-}C_4H_3NMe)(CO)_{10}]$ (**5**) showning the vertical $\eta^1$-bridge.

Table 3

Selected bond lengths (Å) and angles (°) for the cluster $[Os_3(\mu\text{-}H)(\mu\text{-}C_4H_3NMe)(CO)_{10}]$ (5)

| | | | |
|---|---|---|---|
| Os(1)–Os(2) | 2.762(1) | Os(2)···N(1) | 3.21(2) |
| Os(1)–Os(3) | 2.868(1) | C(1)–C(2) | 1.42(3) |
| Os(2)–Os(3) | 2.871(1) | C(2)–C(3) | 1.39(3) |
| Os(1)–C(1) | 2.26(2) | C(3)–C(4) | 1.40(4) |
| Os(2)–C(1) | 2.25(2) | C(4)–N(1) | 1.29(3) |
| Os(2)···C(2) | 3.19(2) | C(5)–N(1) | 1.50(3) |
| Os(1)···C(2) | 3.19(2) | C(1)–N(1) | 1.42(3) |
| Os(1)···N(1) | 3.17(2) | | |
| Os(1)–Os(2)–Os(3) | 61.2(1) | Os(2)–Os(1)–C(1) | 52.0(5) |
| Os(1)–Os(3)–Os(2) | 57.5(1) | Os(1)–C(1)–Os(2) | 75.6(6) |
| Os(2)–Os(1)–Os(3) | 61.3(1) | Os(1)–C(1)–C(2) | 119(2) |
| Os(3)–Os(1)–C(1) | 92.5(5) | Os(2)–C(1)–C(2) | 119(1) |
| Os(3)–Os(2)–C(1) | 92.6(6) | Os(1)–C(1)–N(1) | 118(1) |
| Os(1)–Os(2)–C(1) | 52.3(6) | Os(2)–C(1)–N(1) | 121(2) |

destabilised. Accordingly we reacted $[Os_3(CO)_{10}(MeCN)_2]$ with *N*-methylindole and obtained a compound of the correct stoichiometry, $[Os_3(H)(C_9H_5NMe)(CO)_{10}]$ (**6**). The crystal structure was determined and this showed that we had formed neither **I** nor **J** because the metallation had occurred at the 3-position to give cluster **6** as shown in Fig. 8. Selected bond lengths and angles of **6** are given in Table 4. The

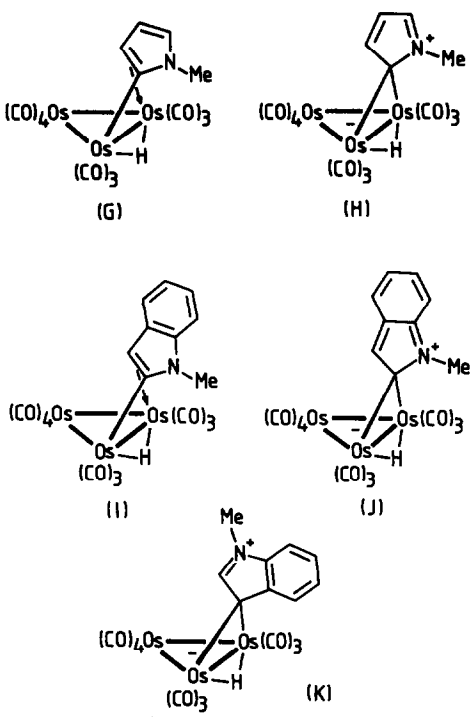


Fig. 7. Two possible descriptions of the cluster $[Os_3(\mu\text{-}H)(\mu\text{-}C_4H_3NMe)(CO)_{10}]$ (**5**) with $\eta^2$ (**G**) and $\eta^1$ (**H**) coordination and possible related structures from *N*-methylindole.

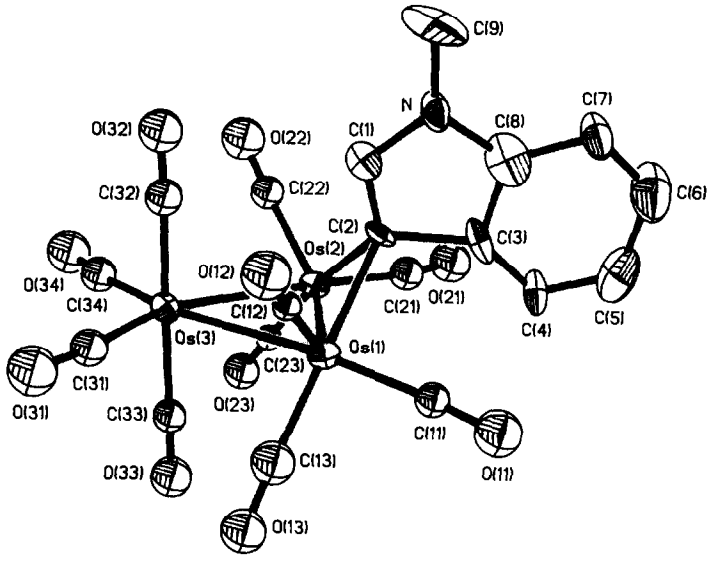


Fig. 8. Molecular structure of the *N*-methylindolyl cluster $[Os_3(\mu\text{-}H)(\mu\text{-}C_6H_4C_2HNMe)(CO)_{10}]$ (**6**).

vertical $\eta^1$-mode of bonding as in **K** has been adopted since the benzo ring now lies across what is formally a double bond and a quinoidal arrangement is not required. The dihedral angle between the $Os_3$ ring and the $C_4N$ ring is 86.0°.

Results presented in this paper indicate that these heterocyclic compounds can adopt structures corresponding to either of the vinyl forms **C** or **D** in Fig. 1. Previously we have shown that **C** and **D** are only extremes of a continuum of accessible structures [4]. Figure 9 shows the obvious relationship that should exist between angle $\theta$ and the distance Os–C($\beta$) for a range of vinyl complexes of type $[Os_3(\mu\text{-}H)(\mu\text{-}CHCHR)(CO)_{10}]$ for which the crystal structures are known. While it is not surprising that these parameters are related, the range and distribution of

Table 4

Selected bond lengths (Å) and angles (°) for the cluster $[Os_3(\mu\text{-}H)(\mu\text{-}C_8H_5NMe)(CO)_{10}]$ (**6**)

| | | | |
|---|---|---|---|
| Os(1)–Os(2) | 2.769(2) | Os(2) · · · C(3) | 3.26(4) |
| Os(1)–Os(3) | 2.860(2) | C(1)–C(2) | 1.32(5) |
| Os(2)–Os(3) | 2.867(3) | C(2)–C(3) | 1.60(5) |
| Os(1)–C(2) | 2.24(4) | C(3)–C(8) | 1.46(7) |
| Os(2)–C(2) | 2.26(4) | C(8)–N | 1.45(6) |
| Os(1) · · · C(1) | 3.12(4) | C(1)–N | 1.38(5) |
| Os(2) · · · C(1) | 3.22(4) | C(9)–N | 1.44(6) |
| Os(1) · · · C(3) | 3.18(4) | | |
| Os(1)–Os(2)–Os(3) | 60.9(1) | Os(2)–Os(1)–C(2) | 52(1) |
| Os(1)–Os(3)–Os(2) | 57.8(1) | Os(1)–C(2)–Os(3) | 76(1) |
| Os(2)–Os(1)–Os(3) | 61.2(1) | Os(1)–C(2)–C(1) | 120(3) |
| Os(3)–Os(1)–C(2) | 91.5(9) | Os(2)–C(2)–C(1) | 126(3) |
| Os(3)–Os(2)–C(2) | 91(1) | Os(1)–C(2)–C(3) | 111(2) |
| Os(1)–Os(2)–C(2) | 52(1) | Os(2)–C(2)–C(3) | 114(2) |

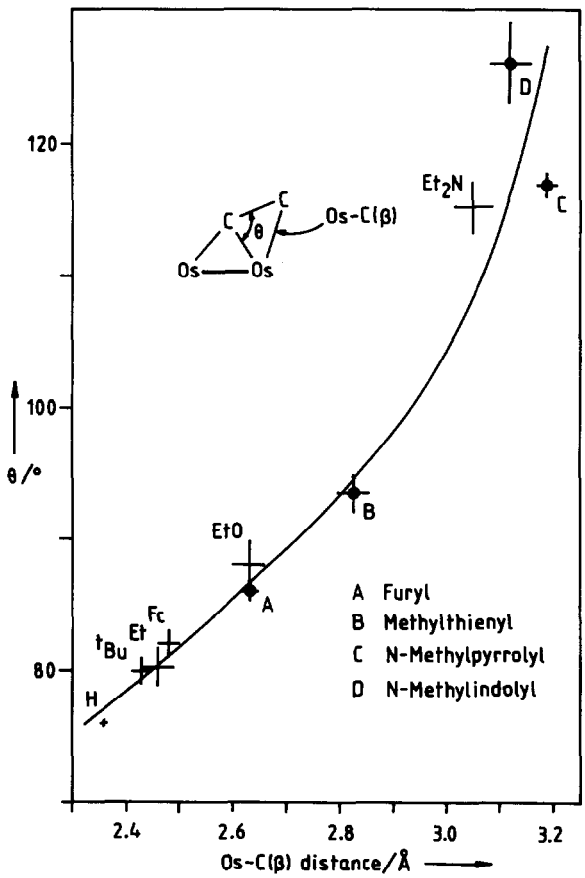


Fig. 9. The relationship between angle $\theta$ and the Os–C($\beta$) distance in the compounds $[Os_3(\mu\text{-H})(\mu\text{-CHCHR})(CO)_{10}]$ where the group R is H, $^t$Bu, Et, Fc, OEt, or $NEt_2$. The additional points A to D are for the heterocyclic compounds $[Os_3(\mu\text{-H})(\mu\text{-X})(CO)_{10}]$ where X is the heterocyclic ligand named above.

values for these data show that there are molecules that lie well in between the extremes found for R = H or $NEt_2$. We have included on the graph data points A to D for the heterocyclic compounds discussed in this paper. Whereas points A and B are approximately in the middle, the ligands still $\eta^2$ but well distorted towards $\eta^1$ coordinated, points C and D are close to that of the $\eta^1$-CHCHNEt$_2$ complex. The 10 compounds included in Fig. 9 do seem to form a coherent set.

We have also shown that the change of structure of the vinyl complexes from **C** to **D** (Fig. 1) is correlated with a lowering of the carbonyl stretching wavenumber as a charge separation occurs with a build-up of negative charge at the metal atoms [4]. Figure 10 shows a lower curve for the acyclic vinyl compounds which is approximately parallel with the upper curve for the heterocyclic compounds. Not many data are available for the heterocyclics so we might be overinterpreting but the heterocyclic systems do seem to give a related data set at higher wavenumbers. The appearance of two curves might result from the heteroatom being bonded to the $\alpha$-carbon atom in the heterocyclic compounds but to the $\beta$-carbon atom in the acyclic vinyl compounds. The inductive effect of the heteroatom closer to the metal

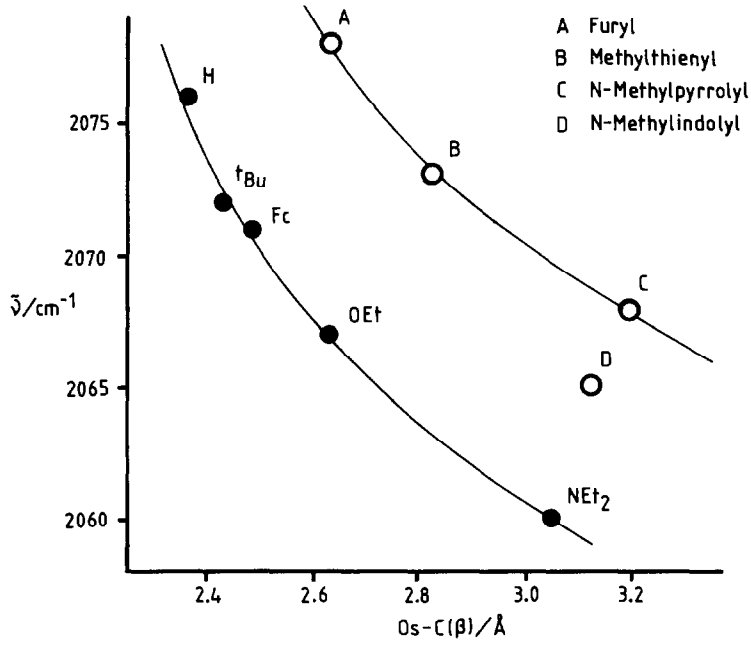


Fig. 10. Graph of $\tilde{\nu}$, the average of the three highest wavenumber carbonyl absorptions which are easily picked out, against the distance Os–C($\beta$) as defined in Fig. 9. The points for the acyclic systems $[Os_3(\mu\text{-H})(\mu\text{-CHCHR})(CO)_{10}]$ are filled (●) whereas those for the heterocyclic compounds are open (○).

atoms would presumably be stronger and lead to higher wavenumbers. Whatever the explanation for the difference between the two curves, there is no reason for them to coincide because the systems are significantly different. Note that point D for the *N*-methylindolyl compound corresponds to a heterocyclic system with the heteroatom in the same relative position as the group R in the compounds forming the lower curve. The variation of wavenumber in Fig. 10 is not large and perhaps some other physical parameter such as ionization energy would make a better correlation. We predict that the data for the compound $[Os_3(\mu\text{-H})(\mu\text{-CHCHSEt})(CO)_{10}]$, not yet synthesised, should lie on the lower curve between OEt and $NEt_2$ approximately below point B.

## Experimental

*Reactions of heterocyclic compounds with $[Os_3(CO)_{10}(MeCN)_2]$*

*Furan.* Following the method of Himmelreich and Müller [7], we synthesised the furyl cluster $[Os_3(\mu\text{-H})(\mu\text{-}C_4H_3O)(CO)_{10}]$ (**3**) and by essentially the same route the new 2-methylfuryl derivative $[Os_3(\mu\text{-H})(\mu\text{-}C_4H_2MeO)(CO)_{10}]$ (**4**).

*Thiophene.* A solution of the bis-acetonitrile cluster (0.170 g) and purified thiophene (1.0 $cm^3$) in cyclohexane (40 $cm^3$) was refluxed under nitrogen for 30 min. The orange-red residue after the removal of solvent under reduced pressure was separated by careful TLC ($SiO_2$; eluant: pentane/dichloromethane (10/1 v/v)) to give three bands of which only two gave enough material to characterise as

$[Os_3(\mu\text{-H})(\mu\text{-}C_4H_3S)(CO)_{10}]$ (**1**) as a deep-red solid (0.097 g, 57%) and $[Os_3(\mu\text{-H})_2(\mu_3\text{-}C_4H_2S)(CO)_9]$ as pale-yellow crystals (0.017 g, 10%) [9].

*2-Methylthiophene.* A solution of $[Os_3(CO)_{10}(MeCN)_2]$ (0.150 g) and 2-methylthiophene (1.0 $cm^3$) was heated under reflux under nitrogen for 20 min. Removal of the solvent under reduced pressure and TLC of the orange residue ($SiO_2$; eluant: n-hexane) gave one red-orange band characterised as $[Os_3(\mu\text{-H})(\mu\text{-}C_4H_2MeS)(CO)_{10}]$ (**2**) as red crystals (0.076 g, 50%). Evaporation of a hexane solution gave crystals suitable for single-crystal X-ray structure determination.

*N-Methylpyrrole.* A solution of $[Os_3(CO)_{10}(MeCN)_2]$ (0.100 g) and *N*-methylpyrrole (1.0 $cm^3$) in cyclohexane (50 $cm^3$) was heated under reflux for 30 min. The orange-red residue after removal of the solvent under reduced pressure was separated by TLC ($SiO_2$; eluant: petroleum ether (b.p. 40–60 °C)) to give three bands

Table 5

Crystal data, details of data collection, structure solution, and refinement for $[Os_3(\mu\text{-H})(\mu\text{-}C_4H_2MeS)(CO)_{10}]$ (**2**), $[Os_3(\mu\text{-H})(\mu\text{-}C_4H_3NMe)(CO)_{10}]$ (**5**) and $[Os_3(\mu\text{-H})(\mu\text{-}C_6H_4C_2HNMe)(CO)_{10}]$ (**6**)

| | **2** | **5** | **6** |
|---|---|---|---|
| Formula | $C_{15}H_6O_{10}Os_3S$ | $C_{15}H_7NO_{10}Os_3$ | $C_{19}H_9NO_{10}Os_3$ |
| *M* | 948.87 | 931.83 | 981.89 |
| Colour | orange-red | red | red |
| Size ($mm^3$) | $0.18\times0.12\times0.28$ | $0.43\times0.42\times0.08$ | $0.30\times0.36\times0.40$ |
| Crystal system | monoclinic | monoclinic | monoclinic |
| Space group | $P2_1/n$ | $P2_1/c$ | $P2_1/c$ |
| *a* (Å) | 10.032(2) | 12.138(2) | 8.718(4) |
| *b* (Å) | 14.976(6) | 12.086(3) | 11.270(6) |
| *c* (Å) | 13.916(5) | 13.532(4) | 23.20(1) |
| $\beta$ (°) | 95.70(2) | 96.45(2) | 95.15(4) |
| *U* ($Å^3$) | 2080(1) | 1972.6(9) | 2270(2) |
| *Z* | 4 | 4 | 4 |
| $D_c$ ($g\,cm^{-3}$) | 3.03 | 3.14 | 2.87 |
| $\mu$(Mo-$K_\alpha$) ($cm^{-1}$) | 184.5 | 193.6 | 168.3 |
| *F*(000) | 1680 | 1648 | 1752 |
| No. orientation reflns.; $2\theta$ range | 27; 11 to 26° | 29; 7 to 26° | 28; 13 to 25° |
| Total no. data | 3998 | 3838 | 4482 |
| No. unique data | 3625 | 3647 | 3971 |
| Rejectn. criterion | $I_0 \le 1.5\sigma(I_0)$ | $I_0 \le 3\sigma(I_0)$ | $I_0 \le 2\sigma(I_0)$ |
| No. data used | 2685 | 2904 | 2589 |
| No. parameters | 262 | 262 | 198 |
| *g* in wght. scheme | 0.00116 | 0.00131 | 0.0023 |
| *R* | 0.0609 | 0.0665 | 0.0771 |
| $R_w$ | 0.0599 | 0.0650 | 0.0781 |
| Max. shift/e.s.d. in last L.S. | 0.002 | 0.007 | 0.005 |
| Max. peak in final diff. Fourier (e $Å^{-3}$) | 2.28 | 4.6 | 3.4 |

[a] All structures: Nicolet R3v/m, Mo-$K_\alpha$ radiation, temp. 23 °C, λ 0.71073 Å, scan mode $\omega-2\theta$, $2\theta$ range: $5 \le 2\theta \le 50°$, data corrected for Lorentz and polarization effects and for absorption by the azimuthal scan method, structure solution direct methods, weight *w* in weighting scheme: $1/[\sigma^2(F)+gF^2]$, $R_w=[\Sigma w(|F_o|-|F_c|)^2/\Sigma w|F_o|^2]^{1/2}$.

of which only one gave enough material to characterise. The product $[Os_3(\mu\text{-H})(\mu\text{-}C_4H_3NMe)(CO)_{10}]$ (**5**) gave orange-red crystals (0.035 g, 35%). Evaporation of a cyclohexane solution gave crystals suitable for X-ray structure determination.

N-*Methylindole.* A solution of $[Os_3(CO)_{10}(MeCN)_2]$ (0.092 g) and *N*-methylindole (0.5 $cm^3$) in cyclohexane (50 $cm^3$) was heated under reflux for 2 h. The brown-orange residue after removal of the solvent under reduced pressure was separated by TLC ($SiO_2$; eluant: pentane/dichloromethane (5/1 v/v)) to give two main bands. A yellow band was characterised as $[Os_3(\mu\text{-H})_2(\mu_3\text{-}C_8H_4NMe)(CO)_9]$ as yellow crystals (0.017 g, 18%) and the main orange band as $[Os_3(\mu\text{-H})(\mu\text{-}C_8H_5NMe)(CO)_{10}]$ (**6**) as orange crystals (0.052 g, 56%). Evaporation of a hot cyclohexane solution gave crystals suitable for single-crystal X-ray structure determination.

*Single-crystal structure determinations for* ***2, 5 and 6***

The single-crystal X-ray structures of the three related compounds were determined using a Nicolet *R3v/n* diffractometer operating with Mo-$K_\alpha$ radiation ($\lambda$

Table 6

Fractional atomic coordinates ($\times 10^4$) for the cluster $[Os_3(\mu\text{-H})(\mu\text{-}C_4H_2MeS)(CO)_{10}]$ (**2**)

| Atom | *x* | *y* | *z* |
|---|---|---|---|
| Os(1) | 1497(1) | 8471(1) | 1954(1) |
| Os(2) | 3509(1) | 8081(1) | 3453(1) |
| Os(3) | 945(1) | 8738(1) | 3910(1) |
| S | 4522(8) | 9004(6) | 1310(5) |
| C(1) | 3392(26) | 9143(18) | 2202(18) |
| C(2) | 4013(24) | 9819(15) | 2801(17) |
| C(3) | 5264(23) | 10084(18) | 2596(19) |
| C(4) | 5704(26) | 9754(21) | 1794(16) |
| C(5) | 6923(29) | 9948(24) | 1394(19) |
| C(11) | 607(30) | 9540(28) | 1522(19) |
| O(11) | 92(25) | 10189(18) | 1250(19) |
| C(12) | 1876(30) | 8101(22) | 699(20) |
| O(12) | 2011(24) | 7796(19) | −31(14) |
| C(13) | −133(27) | 7812(20) | 1905(20) |
| O(13) | −1136(23) | 7454(17) | 1786(15) |
| C(21) | 4490(28) | 8675(18) | 4557(17) |
| O(21) | 5038(22) | 8980(14) | 5197(13) |
| C(22) | 5097(30) | 7551(22) | 2959(17) |
| O(22) | 6013(22) | 7258(17) | 2739(17) |
| C(23) | 3229(36) | 7074(19) | 4258(23) |
| O(23) | 3228(31) | 6457(16) | 4701(21) |
| C(31) | 544(34) | 7448(25) | 3949(21) |
| O(31) | 191(27) | 6733(16) | 4018(17) |
| C(32) | 1265(32) | 10002(19) | 3678(21) |
| O(32) | 1355(26) | 10740(14) | 3521(19) |
| C(33) | 1401(23) | 8794(17) | 5253(18) |
| O(33) | 1729(23) | 8887(15) | 6064(15) |
| C(34) | −973(28) | 8953(20) | 3851(18) |
| O(34) | −2060(23) | 9058(17) | 3833(20) |

Table 7

Fractional atomic coordinates ($\times 10^4$) for the cluster $[Os_3(\mu\text{-}H)(\mu\text{-}C_4H_3NMe)(CO)_{10}]$ (**5**)

| Atom | *x* | *y* | *z* |
|---|---|---|---|
| Os(1) | 3731(1) | 257(1) | 2697(1) |
| Os(2) | 1654(1) | 468(1) | 3327(1) |
| Os(3) | 2079(1) | 1517(1) | 1504(1) |
| N(1) | 2842(16) | −1896(13) | 3692(14) |
| C(1) | 2515(18) | −1098(16) | 2952(17) |
| C(2) | 2057(18) | −1739(16) | 2122(17) |
| C(3) | 2102(24) | −2839(16) | 2428(26) |
| C(4) | 2552(23) | −2883(17) | 3422(19) |
| C(5) | 3351(28) | −1715(21) | 4745(19) |
| C(11) | 4879(22) | −420(16) | 3536(19) |
| O(11) | 5653(16) | −724(15) | 4006(16) |
| C(12) | 4179(19) | −362(20) | 1490(21) |
| O(12) | 4354(19) | −766(16) | 782(14) |
| C(13) | 4615(17) | 1533(15) | 2581(18) |
| O(13) | 5162(15) | 2270(14) | 2553(19) |
| C(21) | 1448(25) | −61(18) | 4635(23) |
| O(21) | 1244(20) | −278(17) | 5398(14) |
| C(22) | 251(19) | 9(18) | 2707(16) |
| O(22) | −623(13) | −251(13) | 2360(16) |
| C(23) | 1063(18) | 1879(14) | 3627(17) |
| O(23) | 719(16) | 2704(14) | 3802(14) |
| C(31) | 2984(22) | 1962(20) | 462(19) |
| O(31) | 3562(15) | 2160(15) | −79(12) |
| C(32) | 1583(26) | 272(19) | 687(20) |
| O(32) | 1268(23) | −381(15) | 116(17) |
| C(33) | 2591(24) | 2760(17) | 2354(19) |
| O(33) | 2891(15) | 3496(14) | 2799(14) |
| C(34) | 692(22) | 2260(17) | 1157(17) |
| O(34) | −135(18) | 2695(16) | 924(16) |

0.71073 Å) at 23°C. Details of the crystal data for $[Os_3(\mu\text{-}H)(\mu\text{-}X)(CO)_{10}]$ (**2**; X = $C_4H_2MeS$), (**5**; X = $C_4H_3NMe$), and (**6**; X = $C_6H_4C_2HNMe$), of the intensity data collections, of the structure solutions and refinements for these clusters are collected in Table 5. For each compound the reflection intensities were corrected for Lorentz and polarization effects and for crystal decay, even though this was minimal, by fitting the data to a curve calculated from the intensities of three standard reflections measured periodically throughout the experiment. Empirical absorption corrections were made by the azimuthal scan method and each structure was solved by direct methods.

For compounds **2** and **5** all non-H atoms were refined anisotropically and the H-atoms of the ligand, but not the hydride, were included in idealised positions with C–H distance fixed at 0.96 Å and isotropic thermal parameters at 0.08 $Å^2$. For compound **6**, which was less satisfactorily refined, all the non-H atoms except the CO ligands were refined anisotropically and no H-atoms were included in the model. Atomic coordinates for the three compounds are in Tables 6 to 8.

Table 8

Fractional atomic coordinates ($\times 10^4$) for the cluster $[Os_3(\mu\text{-}H)(\mu\text{-}C_8H_5NMe)(CO)_{10}]$ (**6**)

| Atom | *x* | *y* | *z* |
|---|---|---|---|
| Os(1) | −5627(2) | 3413(1) | 3996(1) |
| Os(2) | −8756(2) | 3875(1) | 3840(1) |
| Os(3) | −6942(2) | 4125(1) | 2876(1) |
| N | −7855(42) | 134(30) | 4116(13) |
| C(1) | −7664(40) | 1150(34) | 3796(16) |
| C(2) | −7571(49) | 2147(32) | 4095(16) |
| C(3) | −7642(43) | 1796(36) | 4761(17) |
| C(4) | −7647(49) | 2336(38) | 5283(16) |
| C(5) | −7750(62) | 1670(64) | 5772(20) |
| C(6) | −7977(92) | 335(60) | 5727(25) |
| C(7) | −7931(68) | −246(41) | 5205(19) |
| C(8) | −7865(51) | 513(49) | 4711(23) |
| C(9) | −7920(70) | −1057(38) | 3892(28) |
| C(11) | −4812(43) | 3160(33) | 4755(16) |
| O(11) | −4140(40) | 3004(32) | 5206(15) |
| C(12) | −4474(36) | 2231(29) | 3607(13) |
| O(12) | −3840(39) | 1548(31) | 3398(14) |
| C(13) | −4195(60) | 4604(48) | 3908(21) |
| O(13) | −3180(39) | 5269(31) | 3871(14) |
| C(21) | −9975(48) | 3779(37) | 4494(17) |
| O(21) | −10846(40) | 3731(31) | 4810(14) |
| C(22) | −10306(46) | 3284(37) | 3283(17) |
| O(22) | −11185(42) | 2890(34) | 2976(15) |
| C(23) | −9445(37) | 5432(30) | 3686(14) |
| O(23) | −9843(34) | 6421(27) | 3597(12) |
| C(31) | −5203(48) | 4218(37) | 2497(17) |
| O(31) | −4087(43) | 4211(33) | 2220(15) |
| C(32) | −7340(48) | 2543(38) | 2608(17) |
| O(32) | −7472(37) | 1594(29) | 2440(13) |
| C(33) | −6516(44) | 5714(35) | 3168(16) |
| O(33) | −6270(36) | 6654(30) | 3335(13) |
| C(34) | −8522(49) | 4729(39) | 2331(18) |
| O(34) | −9547(42) | 5023(32) | 2047(15) |

All calculations were carried out using a MicroVax II computer using SHELXTL-PLUS [13].

## Acknowledgements

We thank the SERC for an award towards the purchase of the diffractometer.

## References

1 E. Boyar, A.J. Deeming, M.S.B. Felix, S.E. Kabir, T. Adiata, R. Bhusate, M. McPartlin and H.R. Powell, J. Chem. Soc., Dalton Trans., (1989) 5.
2 E. Boyar, A.J. Deeming and S.E. Kabir, J. Chem. Soc., Chem. Commun., (1986) 577; A.J. Deeming, S.E. Kabir, D. Nuel and N.I. Powell, Organometallics, 8 (1989) 717.
3 R.D. Adams and J.T. Tanner, Organometallics, 7 (1988) 2241.

4 A.J. Deeming, M.S.B. Felix, D. Nuel, N.I. Powell, and D.A. Tocher, J. Organomet. Chem., 384 (1990) 181.
5 J.R. Shapley, M. Tachikawa, M.R. Churchill and R.A. Lashewysz, J. Organomet. Chem., 162 (1978) C39; M.R. Churchill and B.G. de Boer, Inorg. Chem., 18 (1979) 848.
6 A.J. Arce, A.J. Deeming, Y. De Sanctis, R. Machado, J. Manzur and C. Rivas, J. Chem. Soc., Chem. Commun., (1990) 1568.
7 D. Himmelreich and G. Müller, J. Organomet. Chem., 297 (1985) 341.
8 M. Choi and R.J. Angelici, J. Am. Chem. Soc., 112 (1990) 7811.
9 A.J. Arce, Y. De Sanctis, A.J. Deeming, M. Day and K.I. Hardcastle, Organometallics, 9 (1990) 6.
10 A.G. Orpen, A.V. Rivera, E.G. Bryan, D. Pippard, G.M. Sheldrick and K.D. Rouse, J. Chem. Soc., Chem. Commun., (1978) 723.
11 A.G. Orpen, D. Pippard and G.M. Sheldrick, Acta Crystallogr., Sect. B, 34 (1978) 2466.
12 A.D. Clauss, M. Tachikawa, J.R. Shapley and C.G. Pierpont, Inorg. Chem., 20 (1981) 1528.
13 G.M. Sheldrick, SHELXTL-PLUS, An integrated system for refining and displaying crystal structures from diffraction data, University of Göttingen, 1986.